PHYSICAL REVIEW D **96,** 064033 (2017)

When black holes collide: Probing the interior composition by the spectrum of ringdown modes and emitted gravitational waves

Ram Brustein,[1,*] A. J. M. Medved,[2,3†] and K. Yagi[4,‡]

[1]*Department of Physics, Ben-Gurion University, Beer-Sheva 84105, Israel*
[2]*Department of Physics & Electronics, Rhodes University, Grahamstown 6140, South Africa*
[3]*National Institute for Theoretical Physics (NITheP), Western Cape 7602, South Africa*
[4]*Department of Physics, Princeton University, Princeton, New Jersey 08544, USA*

(Received 8 May 2017; published 22 September 2017)

The merger of colliding black holes (BHs) should lead to the production of ringdown or quasinormal modes (QNMs), which may very well be sensitive to the state of the interior. We put this idea to the test with a recent proposal that the interior of a BH consists of a bound state of highly excited, long, closed, interacting strings; figuratively, a collapsed polymer. We show, using scalar perturbations for simplicity, that such BHs do indeed have a distinct signature in their QNM spectrum: A new class of modes whose frequencies are parametrically lower than the lowest-frequency mode of a classical BH and whose damping times are parametrically longer. The reason for the appearance of the new modes is that our model contains another scale, the string length, which is parametrically larger than the Planck length. This distinction between the collapsed-polymer model and general-relativistic BHs could be made with gravitational-wave observations and offers a means for potentially measuring the strength of the coupling in string theory. For example, GW150914 already allows us to probe the strength of the string coupling near the regime which is predicted by the unification of the gravitational and gauge-theory couplings. We also derive bounds on the amplitude of the collapsed-polymer QNMs that can be placed by current and future gravitational-wave observations.

DOI: 10.1103/PhysRevD.96.064033

I. INTRODUCTION AND SUMMARY OF RESULTS

The narrative of classical general relativity (GR) is that the interior of a Schwarzschild black hole (BH) is a region of empty space surrounding a classically singular center. Recently, this picture was understood to be in contradiction with the laws of quantum mechanics and thus revealed as misleading. The modern alternative scenario is that the interior does not exist and spacetime comes to an abrupt end at the BH horizon—either physically as in the fuzzball model of BHs [1–4] (also [5] and, more recently, [6]) or effectively as a "firewall" of high-energy particles surrounding the horizon [7] (also [8–10]). This scenario suggests that at least the near-horizon state (and perhaps the whole interior) has to deviate substantially from the vacuum; a situation that differs greatly from the expectations of GR. The degree of deviation is still under debate.

Here, we will be adopting a model of a Schwarzschild BH for which the interior is not mostly empty, in stark contrast to the GR case. The BH interior rather contains a particular state of matter: a nonclassical, bound state of long, closed, highly excited, interacting strings; in essence, a collapsed polymer [11]. A more figurative way of describing the bound state might be as a "quantum star" consisting of hot fundamental strings in the Hagedorn phase or simply as a "string ball." A more detailed account of this collapsed-polymer model is provided in the Appendix, see Appendix A 1. The polymer's outer surface acts just like a classical BH horizon in the limit $\hbar \to 0$; that is, the interior and exterior are causally disconnected in that enclosed matter had no opportunity to escape from the interior. However, this is only approximately true once quantum effects have been "turned on" [12].

We have argued elsewhere that the low occupation numbers of the Hawking radiation along with the assumption of a unitary theory necessitates a strongly nonclassical state of matter within the BH interior [13–15]. Given such a state, a geometric mean-field description in terms of a metric and other spacetime fields is no longer feasible. But then, faced with the absence of an effective description of the geometry, what can one actually say about the interior of a Schwarzschild BH and its influence on the exterior? We will eventually show that the composition of the interior does indeed become relevant in the context of BH mergers.

Some of our results are expected to hold in general for BH-like objects. For us, "BH-like objects" represents a collective name for exotic spacetimes containing ultracompact objects that can mimic some of the basic properties of a BH as viewed by an external observer but without conforming to the picture from GR (mostly empty space with a dense, singular core). These objects include, for

*ramyb@bgu.ac.il
†j.medved@ru.ac.za
‡kyagi@princeton.edu

example, wormholes, gravastars, firewalls, fuzzballs, graviton condensates, boson stars, neutron stars with a certain equation of state or an anisotropic pressure and, of course, collapsed polymers. Some of the objects, such as boson stars, do not possess an essential property of BHs: a horizon (even an effective one), meaning a bounded region of spacetime from which matter cannot escape classically.

But, as far as we are aware, any known form of matter cannot support such Schwarzschild-sized objects without collapsing under the influence of gravity [16,17]. This is because all known interactions of standard matter are weaker than gravity under these circumstances. Only highly excited string matter seems to be capable of supporting compact enough objects with the properties of a BH and yet not collapse any further. This is the impetus for our current focus on the polymer model; nevertheless, a companion paper [18] considers a more general class of (rotating) BH-like objects.

Our objective is to show how gravitational waves (GWs) can be used as a means for distinguishing the collapsed-polymer model from classical BHs and from other BH-like objects. An observable signal of GWs can be produced from the merger of two colliding BHs. Such an event proceeds in three stages: the inspiral (or premerger), merger and postmerger (or ringdown) stages. In the last of these, the newly formed BH will settle down by emitting ringdown modes—also known as quasinormal modes (QNMs)—which are physically realized in the form of GWs. Note, however, that our analysis uses scalar perturbations for simplicity.

It would be difficult to use the early part of the inspiral stage to discriminate various BH-like models because its binary components are adequately described by point particles. On the other hand, one could, in principle, use the tidal information which is encoded in the later part of the inspiral stage to probe BH-like objects [19–23]. More dominant effects in terms of post-Newtonian order counting for the purpose of probing exotic compact objects include the quadrupole moment [24] and tidal heating at the horizon [25]. But the merger phase is complicated by its highly nonlinear evolution. Moreover, we currently lack merger simulations of binary BH-like objects (except for boson stars [26,27]) that would enable us to probe the merger stage for these exotic spacetimes. Fortunately, the postmerger stage can provide us with an excellent opportunity for detecting QNMs, thanks to the recent advances in GW observations and the promise for future detections [28–31]. A discussion on QNMs can be found in Appendix A 2.

A. Previous work on constraining exotic spacetimes from GW150914

Let us recall here the analysis of the famous merger event GW150914 by the LIGO and Virgo collaborations [28], as well as an associated analysis which constrains possible exotic spacetimes [31–34].

It is generally fair to say that the constraints, in cases for which they apply, are currently weak. The statistical significance in the detection of the merger comes mostly from the premerger and merger phases, whereas that of the ringdown phase is not so useful. What little is known about the ringdown phase is, however, consistent with GR. But this by itself does not have a strong discriminating power among the predictions of GR and various BH-like candidates because, as discussed in Appendix A 2, a sufficiently compact object should be able to produce modes that closely resemble the predominant modes of GR.

Given that the LIGO and Virgo collaborations did not report the presence of a secondary ringdown mode, Yunes and collaborators [34] have placed interesting bounds on the intrinsic dissipation, ringdown frequency $f_{\rm RD}$ and damping frequency $f_{\rm damp}$ of applicable BH-like objects. However, the region of small frequency—our region of interest—was not covered by their analysis.

B. Summary of results

We will show in what follows that the collapsed-polymer model predicts a novel class of low-frequency, long-lived modes. The frequencies of this class are parametrically lower than the GR scale c/R_S (the inverse of the "Schwarzschild time") by a factor of the string coupling g_s; that is, $\omega_R \sim g_s c/R_S$, and the damping times are longer than R_S/c by a factor of the square of the string coupling, $\tau_{\rm damp} \sim 1/g_s^2 R_S/c$. The estimate from the quadrupole formula implies (albeit with less certainty) that the expected strain of the emitted GWs is smaller by a factor of $(g_s^2)^2$ than the strain of the conventional GR modes.

The string coupling is small but, in many string theories and models, it is not "very small." For instance, in string theory, if one requires the unification of the gravitational and gauge-theory couplings, the expectation is $g_s^2/4\pi = 1/25$ or $g_s^2 \simeq 1/2$ [35]. One can just as easily imagine other scenarios in which $g_s^2 \sim 1/100$ or even smaller, but it is not related to any of the extremely small parameters of the BH such as $1/S_{\rm BH}$ ($S_{\rm BH}$ is the BH entropy). Therefore, the value of g_s^2 could easily fall somewhere between $1/2$ and $1/100$. Thus, there is the tantalizing possibility that a mode is detected whose frequency is lower than those of the GR modes, and whose delay in emission time is long enough to be definitive but still short enough to be observationally relevant to future experiments. In this way, there is a characteristic signature for the polymer model that would distinguish it from classical BHs, as well as from some other proposed models (see below).

It is of no coincidence that the string coupling g_s determines the new time (or length) scales. This is a natural outcome for the collapsed-polymer model because it formally introduces the fundamental string length l_s, which then represents a new scale from the perspective of an external observer. Conversely, a hypothetical internal

observer would view the Planck length l_P as the new scale. The string coupling $g_s^2 = (l_P/l_s)^{d-1}$ would then be the sole parameter that could maintain the democracy between the two points of view. In four spacetime dimensions, this is simply the small ratio $g_s^2 = (l_P/l_s)^2 < 1$. The string coupling can then be viewed as the polymer's "dimensionless $\hbar$" $g_s^2 \sim \hbar G_N/l_s^2$.

When it comes to theories of modified gravity like massive gravity, the frequencies of the new modes tend to be larger and the damping times tend to be smaller than their counterparts in GR (e.g., [36]), contrary to what is found here. (Although our basic trends do happen to agree with the quasibound-state modes of these same massive-gravity models, e.g., [37].) Nevertheless, a parametrically longer damping time was also found by the authors of [38] (see also [39–42]) in a related context. Their model is based on the modes being trapped in the inner light ring of a wormhole spacetime, and it is meant to be representative of all BH-like models which are not in possession of a classical BH horizon.

Their enhancement factor for the damping time (with respect to the longest-lived GR mode) scales with a certain power of a log of the ratio between the separation of the wormhole throat from R_s and R_s [43]. Since the exponent is much larger than unity, the scaling effectively follows a power law. On the other hand, our collapsed-polymer model introduces a new length scale l_s and includes an outer surface that acts just like a classical BH horizon when the dimensionless $\hbar$ limits to zero, $g_s^2 \to 0$ [12]. Yet, we find a power law enhancement in the damping time, similar to the findings in [38,43].

Based on how the QNM amplitudes, frequencies and damping times scale with respect to g_s for the polymer model, we are able to use data from GW150914 to derive bounds on the string coupling. This current observation already allows us to probe the string coupling scale in a regime which is close to that predicted by the unification of the gravitational and gauge-theory couplings. Since the g_s^4 scaling in the amplitude is somewhat uncertain, we also derive bounds on the amplitude of the polymer QNMs without assuming such a scaling. We also discuss how the bounds will improve once Advanced LIGO (aLIGO) achieves its design sensitivity.

A couple of final notes: First, since our motivation is to learn about actual astrophysical BHs, we will consider three large, spacelike dimensions ($d = 3$) in mind. Nonetheless, our expectation is that the basic conclusions will persist for any $d > 3$.

Second, we are limiting considerations to Schwarzschild BHs, even though rotating Kerr BHs are more realistic. Nevertheless, as long as a Kerr BH is not too close to extremality, the effects of its rotation on the QNM spectrum of interest should be limited to just subdominant corrections.

Third, a recent complementary paper [18] (which does consider rotating BHs) discusses how a certain class of fluid modes, the Rossby or r-modes, can be used to distinguish classical BHs from any BH-like object that is capable of supporting fluid waves. The proposal there does not, however, discriminate between different BH-like objects.

C. Organization

The rest of the paper is organized as follows: In Sec. II, the Klein-Gordon equation for scalar perturbations is considered, from which the QNM spectrum of collapsed polymers is derived. We go on to explain which modes are the most feasible in terms of GW ringdown observations and emphasize how the amplitude, frequency and damping time of such modes scale with respect to g_s. Next, in Sec. III, we derive both existing and projected bounds on the polymer QNMs with current and future GW observations. Our results are summarized in Sec. IV, followed by an Appendix which contains some background material on the collapsed-polymer model and QNMs.

Before proceeding, we would like to briefly clarify what the collapsed-polymer model is and what it is not. The model arose out of an attempt to reconcile what is known about BHs, their associated paradoxes and the principles of quantum gravity. This led us to conclude that the BH interior is described by a state that must be strongly nonclassical [14]—so much so that it evades a description in terms of semiclassical geometry and, consequently, lacks a metric, field equations, action principle, etc.[1] If this picture seems far fetched, Hawking (among others) has advocated that any description of the interior which is consistent with external observations is as good as any other [44]. The polymer model has so far passed all such tests [11,12], whereas this paper is premised on looking for a new prediction that could be subjected to experimental verification.

II. NEW QUASINORMAL MODES OF THE COLLAPSED-POLYMER MODEL

In general, an ultracompact, relativistic object will produce two classes of QNMs when perturbed: fluid modes and spacetime modes (see Sec. A 2 for further discussion). But not so for a classical BH: Because of its strictly opaque horizon and lack of interior matter, only the latter class is of any relevance. Now, as shown in [12], the outer surface of a polymer BH behaves like a real BH horizon for all practical purposes. In the strict classical limit of $\hbar = 0$—which for the polymer BH is equivalent to setting $g_s^2 = 0$—the interior matter has no chance of escaping. The polymer BH should then, to very good approximation, agree with classical GR as far as the QNM spectrum of the spacetime

[1]We also concluded that the interior has the same equation of state as a hot bath of long, closed strings [11]. Moreover, either of these properties seems to imply the other.

modes is concerned. So our objective is clear: To calculate and then interpret the spectrum for the fluid modes when the object's interior is described by the collapsed-polymer model with a nonvanishing g_s^2.

This condition of $g_s^2 > 0$ is pivotal to "stuff" being able to leak out of the polymer BH in spite of its effective horizon. If the strings are indeed interacting, there is no reason that smaller strings cannot break off from the long loops and then escape if they are close enough to the outer surface to avoid subsequent interactions. This process, being a perturbative quantum effect, is of course suppressed. One of the goals of this section is to determine the degree of this suppression, which can be calculated using Einstein's quadrupole formula and knowledge about the mode frequencies.

Our formal analysis begins with an appropriate form of the Klein-Gordon equation for the perturbation away from equilibrium of some physical quantity, such as the string entropy density, string energy density and so on. A further condition is that the perturbations can couple to the spacetime fields in the exterior region. Here, it will be sufficient to consider the Klein-Gordon equation for a massless scalar perturbation. Incorporating a nonvanishing angular momentum and/or spin would only complicate the practical calculations without affecting the conclusions at a qualitative level. We are not including any (possible) corrections to the Klein-Gordon equation due to the effects of string interactions, as these would necessarily scale as g_s^2 and thus represent subleading corrections to the d'Alembert operator and induce only small corrections to the solutions. Furthermore, we are effectively adopting an approximation that is akin to a Cowling approximation (i.e., perturbations of the spacetime metric are assumed to be irrelevant to the fluid modes) [45]. It is, however, argued in the second half of the Appendix that this approximation is a consequence of the model in question rather than a freely made choice.

A. Wave equation and solutions

It should be kept in mind that the "job" of the polymer is to imitate a Schwarzschild BH. It must then be a spherically symmetric distribution of (stringy) matter with an outermost (gyration) radius of $r = R_S$.

The model-dependent input is the index of refraction $n(\vec{r}) = c/v_{\text{sound}}(\vec{r})$ or, equivalently, the speed of sound $v_{\text{sound}}(\vec{r})$ for the relevant medium. (We now set $c = 1$ except when needed for clarity.) Given our assumption of spherical symmetry, the equation for the perturbation $\Phi(t, r)$ becomes

$$\frac{1}{r^2}\frac{\partial^2[r^2\Phi(t,r)]}{\partial r^2} - [n(r)]^2\frac{\partial^2\Phi(t,r)}{\partial t^2} = 0. \tag{1}$$

Let us reemphasize that Φ is meant to represent the perturbation of a physical quantity (like the entropy density) and that a scalar field has been adopted to simplify the presentation. Equation (1) is the Klein-Gordon equation for flat space such that the coordinates (t, r) are fiducial flat-space coordinates; essentially, labels for the constituent string bits. This choice is unavoidable in the polymer model but, more generally, it is a consequence of the state of the BH interior having to be strongly nonclassical if one insists on unitary evolution [13–15]. The meaning of nonclassicality in this context is that the interior defies a semiclassical geometrical description. One can evade this predicament by adopting the viewpoint that gravity is an emergent inertial force in flat space rather than a manifestation of the curvature of spacetime. This is allowed by virtue of Einstein's equivalence principle.

Let us make one further simplifying assumption that $n(r)$ is constant within the polymer. This may seem to be a rather severe simplification, but it follows from the premise that matter should be distributed uniformly throughout the interior of the polymer [11]. This, in turn, follows from the saturation of certain holographic entropy bounds everywhere inside the polymer [14] which, itself, follows from an argument that the saturation of entropy bounds is a signal of nonclassicality [46]. Now, with this additional assumption, the solutions to Eq. (1) can be expressed as spherical waves,

$$\Phi(t,r) = C_o\frac{e^{-i\omega(t-nr)}}{r} + C_i\frac{e^{-i\omega(t+nr)}}{r}, \qquad r \le R_S, \tag{2}$$

where $C_{o,i}$ are complex constants. Notice that the above solution contains both ingoing and outgoing waves. The latter is a consequence of "quantum leakage," allowing modes to escape outside of the (effective) horizon.

Applying the usual boundary conditions for a standard QNM setup (which are itemized in Sec. A 2), we know that $C_i = -C_o$ because of the constraint $\Phi = 0$ at $r = 0$. We also know that Φ must be matched at the outer surface to the external solution $\tilde{\Phi}$, which is that of a purely outgoing wave,

$$\tilde{\Phi}(t,r) = C_e\frac{e^{-i\omega(t-r)}}{r}, \qquad r \ge R_S, \tag{3}$$

where $n = 1$ has been used for the external vacuum to reflect the fact that massless fields should dominate the outward propagating wave and the Schwarzschild exterior has been ignored because it makes no sense to adopt the emergent-gravity picture on one side of the surface and not on the other for the purpose of matching the two solutions. In any event, this distinction is inconsequential to the subsequent analysis because the properties of interest (the frequencies and damping times) are determined only by the contents and geometry of the interior region (see, e.g., [47]). In effect, the exterior is effectively traced out of the calculation as far as the QNM spectrum is concerned; see Sec. A 2 for further explanation. Hence, in spite of the

qualifier of $r \geq R_S$ in the previous equation, this solution is only strictly true at $r = R_S$. The actual outgoing wave $\tilde{\Phi}(t, r > R_S)$ can be described, from an external point of view, as a superposition of spacetime fields. However, the detailed nature of this superposition is not needed for the problem at hand.

We then need to match the solutions (2) and (3) at the surface $r = R_S$. Since the amplitudes of the solutions are unknown and the time derivatives must match if the solutions already match, this process amounts to the sole condition

$$\left.\frac{\partial_r f}{f}\right|_{r=R_S} = \left.\frac{\partial_r \tilde{f}}{\tilde{f}}\right|_{r=R_S}, \tag{4}$$

where $\Phi(t, r) = e^{-i\omega t} f(r)/r$ and similarly for $\tilde{f}$.

With the redefinition $\omega' = n\omega$, the above matching condition translates into $n = i \tan(\omega' R_S)$, which is solved by [48]

$$\omega'_m = \frac{m\pi}{2R_S} - \frac{i}{2R_S} \ln\left(\frac{n+1}{n-1}\right), \tag{5}$$

where m is any odd integer.

The physical frequencies are then given by

$$\omega_m = \frac{m\pi}{2R_S n} - \frac{i}{2R_S n} \ln\left(\frac{n+1}{n-1}\right), \tag{6}$$

with $m = 1, 3, 5, \ldots$ and it should be kept in mind that $1/n$ is essentially a dimensionless $\hbar$ (this will become evident later). Let us reemphasize that this fluid contribution to the QNM spectrum of the collapsed-polymer BH is *in addition* to the usual spacetime contribution from the BHs of classical GR.

We will encounter two important classes of fluid QNMs; one for which $n \sim 1$ (i.e., $v_{\text{sound}} \sim c$) and another for which $n \gg 1$ ($v_{\text{sound}} \ll c$). For the $n \sim 1$ case, Eq. (6) becomes

$$\omega_m \simeq \frac{m\pi}{2R_S} - \frac{i}{2R_S} \ln\left(\frac{2}{n-1}\right). \tag{7}$$

The logarithm in the imaginary part diverges, which is a sign of some problem for this case in the matching of the internal and external solutions. Indeed, going back to the solutions and substituting $n = 1$, one can see that it is not possible to satisfy the boundary conditions at $r = 0$ and $r = R_S$ simultaneously. As a result, the emission of waves for this class of modes is suppressed. Another way to see this is to take the above expression seriously; then the amplitude of the wave is suppressed according to $\lim_{n\to 1}(n-1)^{t/2R_S}$. This suppression does appear to be a general property of relativistic fluid modes, especially relativistic pressure modes, as this phenomenon has also been found in other models [38,39,49–54].

When $n \gg 1$—which is expected for some of the modes, see below—the imaginary part of the frequency now scales with $1/n^2$. This can be shown by expanding the logarithm in terms of $1/n$ to obtain

$$\omega_m = \frac{m\pi}{2R_S n} - i\left[\frac{1}{R_S n^2} + \mathcal{O}\left(\frac{1}{n^4}\right)\right]. \tag{8}$$

The conclusion is that the subrelativistic modes can couple to the outer spacetime, leaking out at a rate that is determined by $\omega_I \propto v^2_{\text{sound}}/c^2$. Since the leakage has a quantum origin, we may also view v^2_{sound}/c^2 as the polymer's dimensionless $\hbar$ (see below). The amplitude of the leaking modes is, however, similar in magnitude to their amplitude inside the horizon, $|C_e|^2 \simeq |C_o|^2$, as a complete matching process reveals. The above conclusion applies to any partially open, spherically symmetric, very massive system with a uniform index of refraction. The only remaining issue is to identify the velocity of sound for the various subrelativistic modes.

B. Sound velocities in the collapsed polymer

For the collapsed-polymer model, one encounters a number of different mode classes according to the polymer's (or string theory's) hierarchy of parameters. How this comes about is the next topic of discussion.

In general terms, each fluid mode can be attributed to a particular restoring force which can act on a deformed element of fluid. As such, the sound velocity of a mode is determined by

$$(v^2_{\text{sound}})_I = \frac{K_I}{\rho}, \tag{9}$$

where ρ is the energy density and K_I is the elastic modulus corresponding to modes of type I. Different types include pressure modes, bending modes, shear modes, fracture modes, etc. The moduli K_I have dimensions of energy density and scale as $K_I \sim \frac{f_I/A}{\Delta L/L} = \frac{f_I L}{A \Delta L}$, where f_I/A is the corresponding force per unit area and $\Delta L/L$ is the fractional deformation.

Let us recall that a force can be obtained from the derivative of a free energy F with respect to some geometric quantity having a dimension of length. It follows that each modulus K_I can be interpreted as a correction to the free energy per unit volume $\Delta F_I/V$. In other words,

$$K_I = \frac{\Delta F_I}{V}, \tag{10}$$

and then

$$(v^2_{\text{sound}})_I = \frac{\Delta F_I}{V\rho} = \frac{\Delta F_I}{E}, \tag{11}$$

where E is the energy any ΔF_I should be regarded as non-negative.

Let us now apply Eq. (11) to the collapsed-polymer model. Like most any physical quantity in a string theory, the contributions to the polymer's free energy can be sorted out as an expansion in both the Regge slope α' and the string coupling g_s^2 except that, in the language of the polymer model, $\epsilon = l_s/R_S$ inherits the role of α'.[2] Importantly, the condition $\epsilon \ll g_s^2 \ll 1$ is required for the self-consistency of the polymer model [11]. [For a more sophisticated explanation of how all this works, see Sec. A 1 and Eqs. (A8) and (A9) in particular.]

Identifying each order in the expansion as the correction due to a different mode, we can write the leading correction to the "tree-level" free energy $F_0 \sim M_{\rm BH}$ ($M_{\rm BH}$ is the polymer/BH mass) as $\Delta F_1 \sim g_s^2 F_0$. Then $\Delta F_2 \sim \epsilon F_0$, $\Delta F_3 \sim g_s^4 F_0$ and so on. Each of the corrections, including the zeroth-order term, can be expected to correspond to some independent class of modes; some examples are discussed below.

The speed of sound in the stringy interior can be read off of Eq. (11) for any of the modes. For instance, since $F_0 \approx M_{\rm BH} = E$, the corresponding mode is a relativistic wave, $v_{\rm sound} = 1$. The pressure (p) modes, which are associated with volume deformations of the interior, are an example of relativistic waves. This conclusion is based on the observation that $p = \rho$ for a highly excited state of closed strings; this is a well-known result [55] and also follows from Eq. (A7) in the Appendix. Consequently, the bulk modulus for the polymer is $K_B = \rho \frac{dp}{d\rho} = \rho$, from which $(v_{\rm sound}^2)_B = K_B/\rho = 1$ follows. To sum up, the pressure modes and their analogues are based on leading-order changes to the effective free energy and have a speed of sound of $v_{\rm sound} = 1$. As argued earlier, such relativistic modes effectively decouple from the outer region of spacetime and cannot be used to probe the inner structure of the BH.

A more interesting class of modes is that for which the free-energy correction scales as $\Delta F_1 \sim g_s^2 F_0$; these being the leading-order nonrelativistic modes. For this class, $v_{\rm sound}^2 = g_s^2 c^2$ and the frequency of emitted GWs then scales as $\omega \sim v_{\rm sound}/R_S \sim g_s c/R_S$, whereas the damping time due to mode leakage to the outside scales as $\tau_{\rm damp} \sim (1/g_s^2)(R_S/c)$ as follows from Eq. (8). Here, one can see explicitly that $g_s^2 = v_{\rm sound}^2/c^2$; and so both of our estimates for the dimensionless $\hbar$ coincide, with one coming from first principles (see Sec. II. B) and another by estimating the amount of leakage from the horizon (see Sec. II. A).

By counting powers of the coupling g_s^2 and powers of the number of string "bits" N ($N = S_{\rm BH} \sim M_{\rm BH}/\epsilon$) in the free-energy correction $\Delta F_1 \sim g_s^2 N \epsilon$, one can attribute this class of modes to the splitting and subsequent rejoining interactions of single loops of strings. The reasoning behind this claim is that each splitting has a free energy "cost" of g_s^2, as does each subsequent rejoining. Meanwhile, the single factor of N implies that only a single string loop can be involved in any one interaction (as the typical length of a string loop is of order N in string units [56,57]). A physical example from this class is a fracture mode, whereby a "cracklike" defect propagates in the stringy material due to the continual splitting and rejoining of strings.

Other, higher-order classes of modes are less interesting because they are associated with extremely nonrelativistic speeds of sounds (recall that $\epsilon \ll g_s^2$), rendering the frequencies too slow to be relevant in any realistic situation. Nevertheless, it is still interesting to ask about the physical meaning of these classes. For example, those associated with $\Delta F \sim \epsilon^2 F_0$ would include bending modes. This is because the (free) energy "cost" for bending scales as the spacetime curvature, $\Delta F_{\rm bend} \sim F_0/R_S^2 \sim F_0 \epsilon^2$. In a sense, these modes also decouple from the exterior but for a different reason than the pressure modes.

All classes of modes are also subject to intrinsic dissipation. To estimate the strength of this dissipation, we will assume that it is caused by the shear viscosity η. This is because we have a good understanding of the scaling properties of the shear viscosity for the collapsed-polymer model in particular and for BH-like objects in general. Let us start here with an appropriate expression for the rate of intrinsic dissipation $1/\tilde{\tau}$ [58],

$$\frac{1}{\tilde{\tau}} = (\ell - 1)(2\ell + 1) \int_0^{R_S} dr r^{2\ell} \eta \left(\int_0^{R_S} dr \rho r^{2\ell+2} \right)^{-1}, \tag{12}$$

where ℓ is the angular momentum of the mode.

In the case of the polymer model—for which the stringy matter saturates the so-called KSS bound [59] throughout the interior [12]—the relevant expressions are $\rho = 1/(g_s^2 r^2)$ and $\eta = s/(4\pi) = 1/(4\pi g_s^2 r)$ [11], where s is the entropy density. Substituting these into Eq. (12), we then have

$$\begin{aligned} \frac{1}{\tilde{\tau}} &= (\ell - 1)(2\ell + 1) \int_0^{R_S} dr \frac{1}{4\pi} r^{2\ell - 1} \left(\int_0^{R_S} dr r^{2\ell} \right)^{-1} \\ &= \frac{1}{4\pi} \frac{(\ell - 1)(2\ell + 1)^2}{2\ell} \frac{c}{R_S}. \end{aligned} \tag{13}$$

Restricting to the choice $\ell = 2$, as is most relevant to GW production, we finally obtain

$$\frac{1}{\tilde{\tau}} = \frac{25}{16\pi} \frac{c}{R_S}. \tag{14}$$

The result in Eq. (14) applies to relativistic modes. For nonrelativistic modes, the ratio η/ρ scales with $(v_{\rm sound}/c)^2$.

[2]We subsequently work in $l_s = 1$ string units.

This behavior can be understood by starting with the diffusion equation for viscous flow—for which η/ρ serves as the diffusion coefficient—and then making the sound velocity equal to c with the rescaling $r \to (v_{\rm sound}/c)r$. It then follows that

$$\frac{1}{\tilde{\tau}} = \frac{25}{16\pi}\frac{v_{\rm sound}^2}{c^2}\frac{c}{R_S} \tag{15}$$

or, for the fracture modes in particular,

$$\tilde{\tau} = 2\frac{1}{g_s^2}\frac{R_S}{c} \simeq 2\tau_{\rm damp}. \tag{16}$$

So the time scale for intrinsic dissipation is comparable to that of damping.

To summarize, the relativistic modes are "unaware" of the existence of any new physical scale, whereas the fracture modes and their analogues would present a telltale distinction. This contrast can be attributed to the introduction of the string-coupling scale—the ratio l_P/l_s—as its inclusion modifies the spectrum of the fracture modes in a substantial way. The implication is that the QNM spectrum of a collapsed polymer has a definitive and potentially observable signature.

C. Estimate of gravitational-wave emission from polymer black holes

The goal of this subsection is to estimate the relative amplitudes of the emitted GWs and then compare the fracture-mode amplitudes with those due to the spacetime modes. The quadrupole formula can be used to obtain the desired ratio of amplitudes since we know about the respective energies and frequencies of the emitted waves. It should be emphasized that the amplitudes, as estimated here, are much less certain than the frequencies and damping times.

Let us first recall that the (free) energy of a fracture mode scales as $E_{\rm frac} \sim g_s^2 F_0 \sim g_s^2 M_{\rm BH}$, whereas the energy in a GW corresponding to a spacetime mode scales as $E_{st} \sim M_{\rm BH}$. The ratio of energies then scales as

$$\frac{E_{\rm frac}}{E_{st}} \sim g_s^2, \tag{17}$$

where E_{st} can be estimated via observations; for example, in GW150914, GWs carried away about 5% of the total mass of the merging BHs. Let us also recall that the ratio of their squared frequencies scales in the same way, $\omega_{\rm frac}^2/\omega_{st}^2 \simeq g_s^2$.

Now, using the quadrupole formula to estimate the GW strain amplitude h, one finds that the relative amplitudes of the emitted GWs scale according to

$$\frac{h_{\rm frac}}{h_{st}} \simeq \frac{E_{\rm frac}}{E_{st}}\frac{\omega_{\rm frac}^2}{\omega_{st}^2} \simeq (g_s^2)^2, \tag{18}$$

where $Q \sim ER_S^2$ has been used to estimate the *fraction* of the quadrupole moment that contributes to the GW production for each mode. The parameter g_s is expected to be small, but not extremely small, as explained previously.

If the string coupling is indeed not too small, one can anticipate some spectacular observational consequences. For concreteness, let us set $g_s^2 = 1/10$ and choose the other parameters to be those of GW150914—meaning an observed ringdown of $f = 251$ Hz and a damping time (in addition to the standard ringdown time $1/2\pi f \simeq 0.6$ ms) of $\tau = 4$ ms [31]. The new class of GWs is reduced in amplitude by a factor of about $1/100$ in comparison to those already observed but oscillates with frequencies about 3 times lower, $\omega \sim 2\pi(251\ {\rm Hz})/3 \sim 500$ Hz, and has damping times which last about 10 times longer, $\tau \sim 40$ ms. Because of their lengthier ringdown time, the sensitivity for detection of the new class of GWs, as estimated by $h/\sqrt{\rm Hz}$, is enhanced by a factor of $\sqrt{\tau_{\rm damp}} \sim g_s$.[3] This means that the sensitivity for detection has decreased by "only" a factor of g_s^3, rather than the factor g_s^4 as estimated above. Such a g_s^3 scaling in the signal-to-noise ratio (SNR) will be confirmed in the following section.

III. BOUNDS ON POLYMER MODES FROM GRAVITATIONAL-WAVE OBSERVATIONS

We will start off in this section by using the events GW150914 and GW151226 to derive current bounds on the polymer modes. Following this, future projected bounds that are based on the aLIGO design sensitivity will also be derived. A subscript of p or BH is used to distinguish between properties of the polymer modes and classical BH modes respectively.

A. Gravitational-wave spectrum and signal-to-noise ratio

Let us begin here by representing the polymer QNMs as damped, sinusoidal waveforms,

$$h(t) = A_p e^{-(t-t_p)/\tau_p}\sin[2\pi f_p(t-t_p) - \phi_p]\Theta(t-t_p), \tag{19}$$

where Θ is the Heaviside step function, A is a QNM amplitude, f is a QNM frequency and τ is a QNM damping time. Also, t_p is the time delay of the polymer QNM relative to that of a typical GR mode and ϕ_p is a constant phase. The time delay $t_p \sim 1/\omega_p \sim 1/g_s\omega_{\rm BH} \sim \tau_{\rm BH}/g_s$ ensures that these and the classical GR modes will not be superimposed to any significant degree, although this

[3]This enhancement follows from two competing effects: The opportunity for signal detection increasing linearly with time versus the noise increasing only as $\sqrt{t}$. Here, the relevant time scale is the ringdown time.

detectability may deteriorate if one includes the fundamental mode due to possible degeneracies among parameters. The Fourier transform of the above equation works out to be

$$\tilde{h}(f)=e^{2\pi i f t_p}A_p\tau_p\frac{2f_p^2Q_p\cos\phi_p-f_p(f_p-2ifQ_p)\sin\phi_p}{f_p^2-4iff_pQ_p+4(f_p^2-f^2)Q_p^2}, \tag{20}$$

with $Q_p\equiv\pi f_p\tau_p$. The above expression reduces to Eq. (2.2) of [60] when $t_p=0$. Notice as well that $|\tilde{h}|$ does not depend on t_p.

To assist in estimating A_p, we will use $A_p\sim g_s^4A_{\rm BH}$ [cf. Eq. (18)] and thus require the amplitude of the QNMs from a classical BH [61],

$$A_{\rm BH}=\frac{M_{\rm BH}}{r}\mathcal{F}\sqrt{\frac{8\epsilon_{\rm rd}}{M_{\rm BH}Q_{\rm BH}f_{\rm BH}}}, \tag{21}$$

where r is the distance to the source, $\mathcal{F}$ is a function that depends on the source location, $\epsilon_{\rm rd}$ is the ringdown efficiency and $Q_{\rm BH}\equiv\pi f_{\rm BH}\tau_{\rm BH}$. The fitting formula for $f_{\rm BH}$ and $Q_{\rm BH}$ of a BH forming in the aftermath of a binary coalescence of BHs is given in [61]. Here, we are setting the spins of the initial BHs to zero for simplicity. The efficiency is roughly given by $\epsilon_{\rm rd}\approx0.44q^2$ for nonspinning BH binaries [62], where $q\equiv m_1m_2/(m_1+m_2)^2$ is the symmetric mass ratio of a binary with individual masses m_1 and m_2.

Let us now estimate the SNR of collapsed polymers by using [63]

$$\mathrm{SNR}^2=4\int_{f_{\rm min}}^{f_{\rm max}}\frac{|\tilde{h}(f)|^2}{S_n(f)}df, \tag{22}$$

where $f_{\rm min}$ and $f_{\rm max}$ are the minimum and maximum frequency—for which we choose the values $f_{\rm min}=10$ Hz, $f_{\rm max}=3000$ Hz unless otherwise stated—whereas S_n is the detector's noise spectral density. The density S_n for the aLIGO O1 run is given by [64] and the fit can be found in Appendix C of [34], while that for aLIGO's design sensitivity with the zero-detuned, high-power configuration is given in [65].

Figure 1 compares the noise spectral density to the polymer QNM spectrum for various values of g_s^2, with the other parameters chosen to be consistent with GW150914 ($m_1=35.7\,M_\odot$, $m_2=29.1\,M_\odot$, $r=410$ Mpc, $f_{\rm BH}=251$ Hz, $\tau_{\rm BH}=4$ ms [28,31]). We have used the scaling relations $A_p\sim g_s^4A_{\rm BH}$, $f_p\sim g_sf_{\rm BH}$, $\tau_p\sim\tau_{\rm BH}/g_s^2$ as motivated in the previous section and set $\phi_p=0$ for simplicity. The value of $\mathcal{F}$ in Eq. (21) is chosen by requiring that the SNR equals 7 for the case of a classical BH with GW150914 parameters [34,66] [and with $f_{\rm min}=222$ Hz in Eq. (22), which corresponds to the frequency where the spectrum peaks [34]]. We have plotted $2|\tilde{h}|\sqrt{f}$ instead of $|\tilde{h}|$ for the signal spectrum so that the ratio between the signal and noise in Fig. 1 goes roughly as the SNR [cf. Eq. (22)]. Notice that the spectrum's amplitude and width both grow larger as one increases g_s^2.

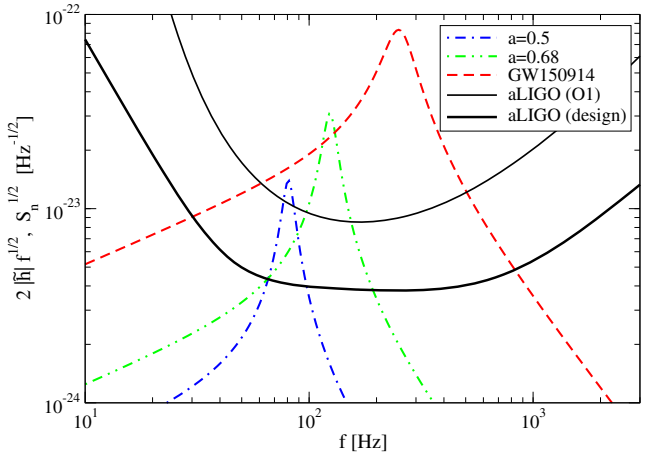

FIG. 1. QNM spectrum of putative polymer modes for GW150914 with various g_s^2, as well as noise spectral density against frequency. For $g_s^2=1$, the QNM amplitude, frequency and damping time for the polymer modes are the same as those of a classical BH. The ratio between the signal and noise roughly corresponds to the SNR. The spectrum is detectable if this ratio is above the threshold (~5).

B. Current and future bounds with gravitational-wave observations

Continuing with the same setup as in the previous subsection, we will next use GW observations to derive bounds on the polymer modes. It will initially be assumed that the QNM amplitude scales with g_s^4 as explained in Sec. II C; however, this assumption will be relaxed later on.

1. Bounds assuming the g_s^4 amplitude scaling

The top panel of Fig. 2 presents the SNR for the QNMs of a collapsed polymer with GW150914 parameters. We have used two aLIGO detectors (corresponding to Hanford and Livingston) with the O1 run. For $g_s^2\sim1$, the SNR scales with g_s^3 as discussed at the end of Sec. II C. This scaling is valid for a white-noise background; however, as g_s^2 becomes smaller, there is an extra suppression due to the frequency dependence of the noise curve. Namely, as one lowers g_s^2, the QNM frequency f_p becomes smaller and enters a range where the detectors are less sensitive (see Fig. 1).

The bottom panel of Fig. 2 depicts the SNR for the case of a collapsed polymer with GW151226 parameters. The value of $\mathcal{F}$ in Eq. (21) is now chosen by requiring that the SNR equals unity for a classical BH with GW151226

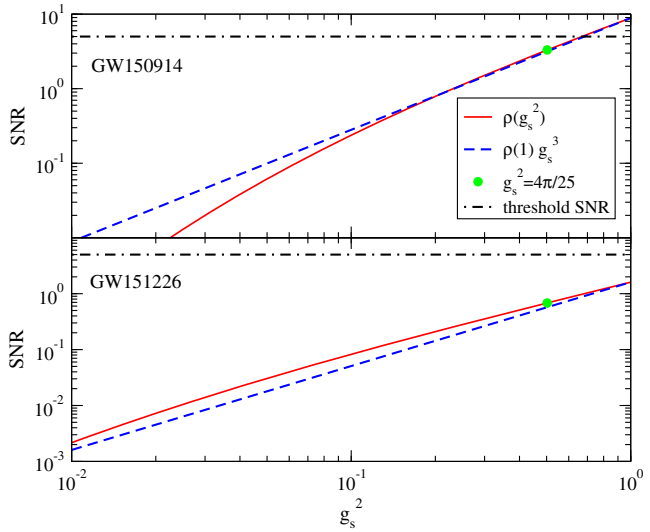

FIG. 2. Top: SNR of the putative QNM of a collapsed polymer for GW150914 as a function of g_s^2 (red, solid). The SNR scales with g_s^3 (blue, dashed) for $g_s^2 \sim 1$ as explained in Sec. II C. The SNR threshold of 5 (black, dot-dashed) allows us to constrain g_s^2 as $g_s^2 \lesssim 0.65$. As the detector sensitivity increases, one will be able to probe g_s^2 for the unification of the gravitational and gauge theory couplings (green dot). Bottom: Same as the top panel but for GW151226.

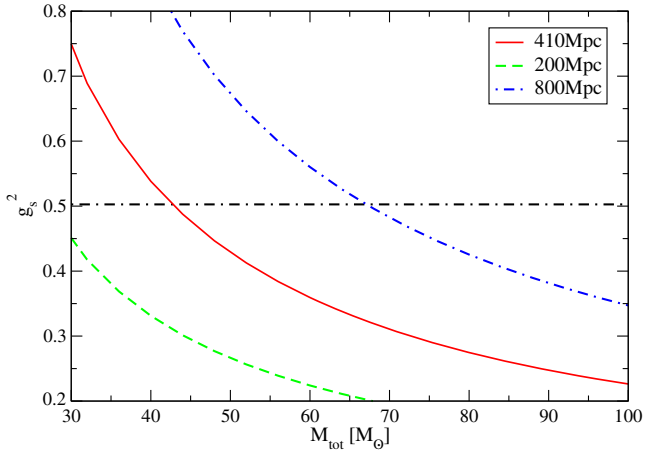

FIG. 3. Projected upper bound on g_s^2 as a function of the total mass of an equal-mass BH binary at various distances apart using aLIGO's design sensitivity. 410 Mpc corresponds to the distance for GW150914 [28]. The horizontal line represents $g_s^2 = 4\pi/25$. The upper bound on g_s^2 scales with $r^{2/3}$.

parameters. The predicted $f_{\rm BH}$ for this source is ∼790 Hz, which is higher than the corresponding frequency in the previous case (251 Hz for GW150914). Consequently, as g_s^2 becomes smaller, f_p is actually entering the region where the detector is *most* sensitive. Meaning that the scaling of the SNR with g_s is shallower than g_s^3.

Let us now derive an upper bound on g_s^2 by using the knowledge that the LIGO-Virgo collaboration did not report the presence of an additional ringdown signal on top of the dominant BH signal.[4] This means that we can derive bounds on the polymer modes under the assumption that the observed data is consistent with gravitational waveforms from binary BH mergers in classical GR. It then follows that the SNR for the polymer modes has to be smaller than the threshold value. For example, if the threshold is 5 [68,69]—as indicated by the horizontal, black, dot-dashed line in the top panel of Fig. 2—one can use GW150914 to roughly bound g_s^2 such that $g_s^2 \lesssim 0.65$ (the upper limit being where the red, solid curve crosses the black, dot-dashed line). This upper bound is intriguingly close to the point where g_s^2 corresponds to the unification of the gravitational and gauge coupling constants, $g_s^2 = 4\pi/25 \sim 0.5$.

It is also interesting to consider the future prospects for constraining g_s^2 with GW observations. Figure 3 displays the projected upper bound on g_s^2 given aLIGO's design sensitivity (again using the two interferometers at Hanford and Livingston) and assuming that aLIGO does not find the collapsed polymer signal. In other words, such an upper bound is equivalent to the *minimum* g_s^2 for which aLIGO would be able to detect such a signal. We have, for concreteness, used the sky-averaged value of $\mathcal{F}$ in Eq. (21), assumed that the initial binary contains equal-mass BHs at various distances r apart and adopted a threshold SNR of 5. As evident from the figure, one can constrain $g_s^2 \lesssim 4\pi/25$ for a total mass of 45 $M_\odot$ or larger when $r = 410$ Mpc. Given that SNR $\propto g_s^3/r$ and that g_s^2 is determined by the SNR being equal to its threshold value, one finds that such an upper bound on g_s^2 is proportional to $r^{2/3}$. We have checked that this analytic scaling in distance agrees with the displayed results in Fig. 3.

The bounds on g_s^2 will further increase as (i) the number of interferometers increases, (ii) the detector sensitivity improves and (iii) one is able to combine signals from multiple sources. We stress that the upper bounds presented here are not robust and should be understood as only rough estimates.

2. Bounds without assuming the g_s^4 amplitude scaling

Since the g_s scaling in A_p is the most uncertain among A_p, f_p and τ_p, it is perhaps more appropriate to place a bound on the relative amplitude $\gamma \equiv A_p/A_{\rm BH}$ without assuming the scaling $A_p \sim A_{\rm BH} g_s^4$. Let us first work out a simple scaling relation for the upper bound on γ. We start with SNR $\propto A_p\sqrt{\tau_p} \propto \gamma A_{\rm BH}/g_s$ and then, like before, require this SNR be equal to its threshold value. On this basis, one finds that the upper bound on γ scales linearly with g_s.

[4]References [40,41] reported the presence of "echoes" on top of the primary ringdown signal. This claim is apparently still in debate [67] as the result has not yet been confirmed by other groups.

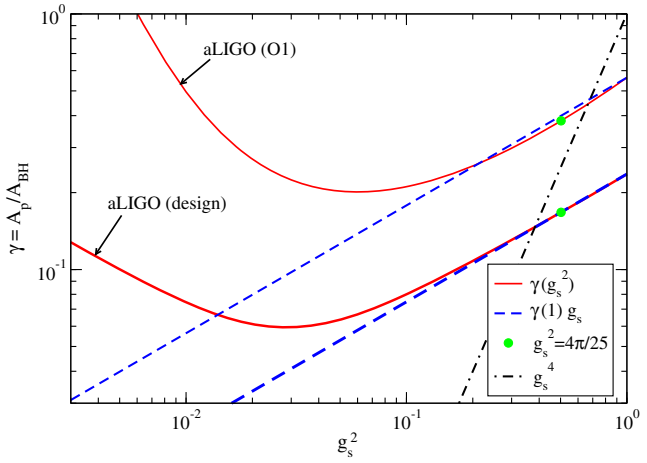

FIG. 4. Upper bound on the relative amplitude γ of the polymer QNMs with respect to the BH QNMs as a function of g_s^2. The thinner red, solid curve is the current bound from GW150914 with aLIGO's O1 run, while the thicker red, solid curve is the projected bound for a GW150914-like event with aLIGO's design sensitivity. Blue, dashed lines are the analytic prediction for the upper bound on γ valid around $g_s^2 = 1$, while green dots are the bounds at $g_s^2 = 4\pi/25$. The black, dot-dashed line is the predicted relative amplitude proportional to the g_s^4 scaling (see Sec. II C).

The thinner red, solid curve in Fig. 4 shows the upper bound on γ from GW150914 with the threshold SNR of 5. These results roughly agree with the linear scaling in g_s, as motivated above, when $g_s^2 \sim 1$ (cf. the uppermost dashed, blue line). The slight deviation from the linear scaling in this regime can be attributed to a small frequency dependence in S_n around $f = f_p$. On the other hand, the curve strongly deviates away from the linear scaling when $g_s^2 \ll 1$. This is because the spectrum falls out of the detector's frequency band as one decreases g_s^2. The GW150914 observation sets $\gamma \lesssim 0.38$ for $g_s^2 = 4\pi/25$. But, if $\gamma = g_s^4$ (see the black, dot-dashed line) as predicted in Sec. II C, then the SNR of the polymer modes for GW150914 becomes smaller than the threshold already when $g_s^2 \lesssim 0.65$—in agreement with the top panel of Fig. 2.

The thicker red, solid curve in Fig. 4 depicts the projected bound on γ when using the noise curve for aLIGO's design sensitivity. One should first observe that the linear-in-g_s scaling near $g_s^2 \sim 1$ is a better fit than that found for aLIGO's O1 run because the noise curve is flatter for the future design sensitivity (see Fig. 1). Second, the upper bound on γ decreases by a factor of ~ 2 at $g_s^2 = 4\pi/25$ in comparison to the current bound from GW150914.

IV. CONCLUSION

We have discussed how the interior structure of BHs, as described by the collapsed-polymer model, affects the spectrum of QNMs. Our main result is the identification of several new classes of QNMs, in addition to the classical GR modes which are a common feature of all BH-like objects with an effective horizon or a light ring [38,39,70–72]. We found subrelativistic modes whose sound velocity is $v_{\rm sound} \simeq g_s c$; these being associated with the self-interactions of the strings. Additionally, there are many other classes of exceptionally slow modes that are induced by weak restoring forces; for instance, one such class describes bending modes with a sound velocity of $v_{\rm sound} \simeq c l_s / R_S$.

We have also discussed how the new classes of QNMs could affect the emission of GWs from BHs. The emission due to relativistic modes is suppressed to such an extent that they essentially decouple from the outer spacetime—in agreement with previous studies in the literature on fluid modes in ultracompact objects. The various classes of exceptionally slow modes are irrelevant because their low frequencies necessitate prohibitively long observation times. Fortunately, the emission due to the leading-order subrelativistic modes was shown to lead to an interesting observable signature: A characteristic ringdown by the emission of low-frequency GWs which follow the conventional emissions after a relatively brief but distinguishable time delay. The amplitude of this new class of GWs is lower than the amplitude of the usual BH GWs by a factor $(g_s^2)^2$.

Our main conclusion is that observations of GWs from colliding BHs provide a means for differentiating the collapsed-polymer model from the BHs of classical GR. These distinctions—the lower frequencies and time delay—are determined mainly by the string coupling, which itself depends on the ratio of the Planck scale to the string scale and is also the dimensionless $\hbar$ for the polymer. Remarkably, we found that GW150914 places an upper bound on g_s^2 that is close to $4\pi/25$, and such a bound will only become stronger as the detector sensitivity improves.

One may still wonder how the fluid modes appear to evade the BH horizon as seen from an external, asymptotic observer's perspective. After all, a horizon must be there as far as *this observer* is concerned, regardless of whether it is a classical BH or merely a BH-like object with an effective horizon. This is an important question in its own right and will be addressed in a separate discussion [73].

ACKNOWLEDGMENTS

We thank Frans Pretorius and Ofek Birnholtz for discussions on the observability of the emitted GW. We also thank John Boguta, Roman Konoplya and Paolo Pani for useful comments on the manuscript. The research of R. B. was supported by the Israel Science Foundation Grant No. 1294/16. The research of A. J. M. M. received support from an NRF Incentive Funding Grant No. 85353 and an NRF Competitive Programme Grant No. 93595. A. J. M. M. thanks Ben Gurion University for their hospitality during his visit. K. Y. acknowledges support from JSPS Postdoctoral Fellowships for Research Abroad, NSF Grant No. PHY-1305682 and Simons Foundation.

APPENDIX: A BRIEF REVIEW ON BACKGROUND

1. The collapsed polymer

The polymer model assumes that the BH interior consists of a hot bath of closed, interacting strings in a finite volume. The properties of such a system are explained in [56,57] (also see [11,12]).

Let us start here by considering a free, highly excited, closed string of length L in an infinite space. In this case, the string occupies a region whose linear size R is given by the random-walk scale, $R \sim l_s\sqrt{L/l_s}$. One can regard $N = L/l_s$ as the total number of "string bits" in the state, and so $R \sim l_s\sqrt{N}$. The situation, however, changes when strings interact, which they do by splitting and joining. Such interactions induce an effective attraction that causes the strings to occupy a smaller region in space, leading to a smaller value of R [74,75]. Since the only relevant scales are l_s and l_P and the strings do not "know" about the latter, one expects that $R \sim l_s N^\nu$ for some ν which could be different than $1/2$. The resulting picture is a finite-sized, bound state of strings that is dominated by about $\ln N$ long loops [56,57].

The parameter N also measures the entropy of the string state and, since $N \sim (R/l_s)^{1/\nu}$, the entropy will not, in general, be extensive. An area law, as in the case of BHs, implies that $\nu = 1/(d-1)$ with d being the number of spatial dimensions. A scaling relation with entropy in terms of R is also described by the Flory-Huggins theory of polymers [76].[5] This theory is reexamined in [79] and reviewed in, for instance, [80]. The parameter ν is called the Flory exponent and the temperature at which the polymer becomes tensionless is known as the Flory temperature. The linear size R is referred to as the gyration radius of the polymer and N represents the total number of monomers within the polymer chain(s). For our case of attractive interactions, the gyration radius is smaller than $l_s\sqrt{N}$ and the system is then identifiable as a "collapsed polymer".

The theory of collapsed polymers has been adopted to show that the bound state of highly excited strings can be described by a quadratic (effective) free energy [11]. In string ($l_s = 1$) units, this free energy F takes the form

$$-\left(\frac{F}{T_{\rm Hag}}\right)_{\rm strings} = \epsilon N - \frac{1}{2}\frac{g_s^2}{V}N^2, \tag{A1}$$

where g_s is the string coupling, $V \sim R^d$ is the occupied volume, $T_{\rm Hag}$ is the Hagedorn temperature and we disregard an order-one numerical factor so that $T_{\rm Hag} = 1$ in string units. The parameter ϵ is an effective, dimensionless temperature which measures the deviation of the actual temperature T from the Hagedorn value, $\epsilon = (T - T_{\rm Hag})/T_{\rm Hag}$. The equilibrium solution of the theory, which is obtained by minimizing the free energy with respect to N, enforces the relation

$$\frac{N}{V} = \frac{\epsilon}{g_s^2}. \tag{A2}$$

The collapsed-polymer scaling relations agree with those of a BH when the parameters of the polymer theory—N, ϵ and g_s^2—are related to those of the BH—the Schwarzschild radius R_S, energy $M_{\rm BH}$ and entropy $S_{\rm BH}$—in a specific way [11]. In particular,[6]

$$R_S = \frac{l_s}{\epsilon}, \tag{A3}$$

meaning that the Hawking temperature is

$$T_{\rm Haw} = \epsilon. \tag{A4}$$

Additionally, the BH entropy is

$$S_{\rm BH} = N = V\frac{\epsilon}{g_s^2} = \left(\frac{R_S}{l_p}\right)^{d-1}, \tag{A5}$$

where l_P is the Planck length, the second equality follows from Eq. (A2) and the last one from $g_s^2 = (l_P/l_s)^{d-1}$ as well as $R = R_S = 1/\epsilon$. Also, the total energy of the bound state is found to be in agreement with that of the BH [cf. Eq. (A7) for the density ρ],

$$E_{\rm bound} = V\frac{\epsilon^2}{g_s^2} = \frac{1}{l_P}\left(\frac{R_S}{l_P}\right)^{d-2} = \epsilon N = M_{\rm BH}. \tag{A6}$$

It is worth noting that the pressure p is equal to the energy density ρ for a highly excited state of closed strings [55]. This equality also follows directly from the free energy (A1), both at and away from equilibrium. Using standard thermodynamics, one finds that the equilibrium values are

$$p = \rho = \frac{\epsilon^2}{g_s^2}. \tag{A7}$$

This pressure is not to be confused with the (effective) tension, $\sigma = \frac{\partial F}{\partial L}$, which vanishes at equilibrium by virtue of $L = l_s N$.

For self-consistency, the string-theory parameters must obey the following relations [11]: $\epsilon \ll g_s^2 \ll 1$ and $g_s^2 N = V\epsilon \gg 1$. Together, these ensure that the BH is large in string units, the coupling is small but finite and the

[5] See the books by De Gennes [77], and Doi and Edwards [78] as well.

[6] Here and for the remainder, the string length l_s, fundamental constants and order-unity numerical factors will only be made explicit when needed for clarity.

higher-order interaction terms in the free energy in Eq. (A1) are suppressed. The higher-order terms can come from $\alpha' \sim l_s^2$ corrections, additional loop corrections or their combination. Because the former is controlled by the Regge slope $\alpha' \propto \epsilon^2$, we know that the equilibrium form of the corrected free energy looks schematically like

$$F \sim \epsilon N[1 + a_1 g_s^2 + a_2 g_s^4 + \cdots] \times [1 + b_1 \epsilon + b_2 \epsilon^2 + \cdots], \tag{A8}$$

where the odd powers of ϵ are shorthand for powers of $g_s^2 N/V$ and originate from loop corrections (the even powers of ϵ could be of either type), whereas the explicit powers of g_s^2 are from string self-interactions. The above hierarchy tells us that the next-to-leading term in the expansion has a suppression factor of g_s^2,

$$F \sim \epsilon N + g_s^2 \epsilon N + \cdots. \tag{A9}$$

When the scaling of the various parameters is appropriately fixed, the bound state appears from the outside to be indistinguishable from a BH. Since this collapsed-polymer model so immaculately replicates the properties of a classical BH (and also those of a semiclassical BH [12]), one might wonder if there is still some property that allows one to distinguish the two descriptions. As shown in the main text, this question can be answered affirmatively by comparing the QNM spectrum of the collapsed-polymer model with the conventional one for the BHs of GR.

2. Quasinormal modes

Just like in the main text, we are limiting considerations to Schwarzschild BHs, even though rotating Kerr BHs are more realistic.

As is now well known (but see [51,52,81] for reviews), a perturbed BH will settle down to its equilibrium state by "ringing" at characteristic complex frequencies which are determined by only a handful of parameters. Since a Schwarzschild BH has only one characteristic scale, the frequencies are determined solely by the horizon radius R_S or, equivalently, the surface gravity $\kappa = 1/(2R_S)$. For both tensor and scalar perturbations, the real parts are of order κ for all modes with low angular momentum $\ell \sim 1$ (otherwise, the frequencies increase, roughly in proportion to ℓ), $\omega_R \equiv \mathrm{Re}\omega \sim \kappa$, whereas the imaginary parts of the frequencies (or the inverses of the damping times) are, to a good approximation, half-integer multiples of the surface gravity, $\omega_I \equiv \mathrm{Im}\omega \approx (m - 1/2)\kappa$ with $m = 1, 2, 3, \ldots$. To be clear, this spectrum has only been established rigorously in the large-m or eikonal limit [82], although a WKB approximation attains roughly the same form at small m [83], as do various numerical studies [51,84].

As shown in the main text, the appearance of a new scale in the polymer model is marked in a specific way in both the real and imaginary parts of the QNM spectrum. It follows that GW frequencies could provide a clear observational distinction between our model and classical BHs.

Two distinct notions of QNMs exist: the "standard" one that is used, for example, in the description of quantum-optics and condensed-matter systems (see, e.g., [47,85]) and there is also the BH notion of QNMs. First, let us discuss the standard case. Here, one is considering an open system that supports waves; for instance, a dielectric or an optical cavity, as either provides a partially reflecting outer surface. Such a system will lose energy to its environment, giving rise to damped (complex-frequency) waves. To determine the QNM spectrum, one is instructed to impose (1) totally reflecting boundary conditions at the center of the system and (2) the condition of purely outgoing waves in the external environment and then, by continuity, the same condition at the outer surface of the system. In effect, the exterior region is traced out of the problem. It is there only for conceptual reasons and plays no essential role from a computational perspective.

The BH notion of QNMs (see, e.g., [51,52]) is different. For a BH spacetime, the problem can be set up like a scattering experiment, which is common in the high-energy literature (e.g., [86]). In this case, one is considering modes that initially came in from infinity and then were either reflected from or transmitted through the Schwarzschild potential barrier (at a radius of about $3/2R_S$). The QNMs can be identified as poles in the scattering amplitude, which is essentially a Fourier transform of the scattering potential. The boundary conditions are those of outgoing waves at spatial infinity and ingoing at the BH horizon. Such a choice of conditions suggests that it is now the interior which is, in effect, traced out, as it always is for an external observer in a BH spacetime. The setup for the BH QNMs is then, in some sense, the mirror image of the standard description.

The simple model of Kokkotas and Schutz [87] demonstrates how these two perspectives can both be accommodated. Those authors describe the interior of some radiating system as a finite string. This string is then coupled by a massless spring to a second, semi-infinite string representing the exterior spacetime. The finite string will generally support two independent classes of modes; one of which is coupled weakly to the exterior and another one, coupled much more strongly. Based on the discussion in [87], one might expect that the modes of the former and latter classes are analogous to modes from the standard and BH perspectives, respectively. This expectation has indeed been verified by studies on ultracompact neutron stars and other (hypothetical) ultracompact, relativistic stars (e.g., [49,50,53,88,89][7]). In these

[7]Many more references can be found in the review articles [51,52].

treatments, one finds that the f- and p-modes (meaning fundamental and pressure modes) are among those associated with the stellar fluid, whereas the so-called w-modes have more resemblance with perturbations in the curvature of spacetime. The separation of the fluid modes from the spacetime modes is known as either the Cowling or inverse Cowling approximation [45,49].

One uses the Cowling approximation when perturbations of the spacetime metric can be neglected. In this case, the strength of the coupling of the fluid modes to the emitted GWs—which in turn determines the amplitude of these emitted waves—can be estimated by way of the celebrated quadrupole formula, which treats the background spacetime as fixed and (essentially) flat [90]. In particular, $h \propto d^2Q/dt^2$, where h is the wave amplitude and Q is the quadrupole moment of the energy density.

The spectrum of QNMs of a BH-like object should be able to at least mimic the predominant modes from the spectrum of its classical GR counterpart. The physical reason for this is that the associated ringdown process depends primarily on the spacetime outside of the ultracompact object, which must be indistinguishable from the exterior spacetime of a BH in GR. (The boundary conditions at the outer surface, which vary from model to model, are also of relevance.) However, if the interior of a BH-like object does contain some matter, then one would expect, as discussed above, some additional (fluid) modes to be excited. Classically, the fluid modes cannot couple to the spacetime modes in the presence of a horizon. However, quantum mechanically, fluid modes would be expected to couple to the spacetime modes by way of "quantum leakage" and then propagate outside of the (would-be) horizon.

Just like for the modes of relativistic stars, the real part of the frequency of a QN fluid mode should be determined by the speed of sound of the interior matter. This velocity is necessarily less than but possibly saturating the speed of light c. For any BH-like object, the spatial scale of the interior is the Schwarzschild radius R_S; otherwise, the object is not sufficiently compact. It is then a generic result that the oscillatory frequency of a mode from this class is bounded from above, $\omega_R \leq c/R_S$. In addition, a time delay of order $1/\omega_R$ in the excitation of a mode can be expected. This is because a waiting time of at least one period is needed for this interior mode to affect the spectrum of QNMs outside of the BH and, therefore, the spectrum of the emitted GWs.

As for the damping time—the inverse of the imaginary part of the frequency $\tau_{\rm damp} = 1/\omega_I$—the situation is less conclusive. On general grounds, one might expect the damping time of a fluid mode to be longer than those of the spacetime modes [88]. To understand why, let us recall the quadrupole formula, which says that the coupling to gravity of such modes is proportional to ω_R^2. Then, since $\omega_R < c/R_S$ is generically true, their coupling must be weaker than it is for the relativistic spacetime modes. On the other hand, the intrinsic dissipation in the fluid could be strong, reducing the damping time.

In our model, the damping time of the matter modes is parametrically larger than $1/\omega_R$, which can be attributed, in part, to the (normalized) intrinsic dissipation being very weak. Because of the weak coupling of these modes to gravity, the emission of GWs will take place over an even longer time scale and thus be a similarly weak source of dissipation. A longer damping time is consistent with the expectations of Cardoso *et al.* [38]. The same authors also stressed the importance of long-time observations in identifying deviations from GR.

[1] S. D. Mathur, What exactly is the information paradox?, Lect. Notes Phys. **769**, 3 (2009).

[2] S. D. Mathur, The information paradox: A pedagogical introduction, Classical Quantum Gravity **26**, 224001 (2009).

[3] S. D. Mathur, What the information paradox is *not*, arXiv:1108.0302.

[4] S. D. Mathur, What does strong subadditivity tell us about black holes?, Nucl. Phys. B, Proc. Suppl. **251–252**, 16 (2014).

[5] K. Skenderis and M. Taylor, The fuzzball proposal for black holes, Phys. Rep. **467**, 117 (2008).

[6] G. t. Hooft, The firewall transformation for black holes and some of its implications, arXiv:1612.08640.

[7] A. Almheiri, D. Marolf, J. Polchinski, and J. Sully, Black holes: Complementarity or firewalls?, J. High Energy Phys. 02 (2013) 062.

[8] N. Itzhaki, Is the black hole complementarity principle really necessary?, arXiv:hep-th/9607028.

[9] S. L. Braunstein, S. Pirandola, and K. Zyczkowski, Entangled Black Holes as Ciphers of Hidden Information, Phys. Rev. Lett. **110**, 101301 (2013).

[10] D. Marolf and J. Polchinski, Gauge/Gravity Duality and the Black Hole Interior, Phys. Rev. Lett. **111**, 171301 (2013).

[11] R. Brustein and A. J. M. Medved, Black holes as collapsed polymers, Fortschr. Phys. **65**, 0114 (2017).

[12] R. Brustein and A. J. M. Medved, Emergent horizon, Hawking radiation and chaos in the collapsed polymer model of a black hole, Fortschr. Phys. **65**, 2 (2017).

[13] L. Alberte, R. Brustein, A. Khmelnitsky, and A. J. M. Medved, Density matrix of black hole radiation, J. High Energy Phys. 08 (2015) 015.

[14] R. Brustein and A. J. M. Medved, Quantum state of the black hole interior, J. High Energy Phys. 08 (2015) 082.
[15] R. Brustein, A. J. M. Medved, and Y. Zigdon, The state of Hawking radiation is non-classical, arXiv:1707.08427.
[16] H. A. Buchdahl, General relativistic fluid spheres, Phys. Rev. **116**, 1027 (1959).
[17] A. Fujisawa, H. Saida, C. M. Yoo, and Y. Nambu, Maximum mass of a barotropic spherical star, Classical Quantum Gravity **32**, 215028 (2015).
[18] R. Brustein, A. J. M. Medved, and K. Yagi, Discovering the interior of black holes, arXiv:1701.07444.
[19] M. Wade, J. D. E. Creighton, E. Ochsner, and A. B. Nielsen, Advanced LIGO's ability to detect apparent violations of the cosmic censorship conjecture and the no-hair theorem through compact binary coalescence detections, Phys. Rev. D **88**, 083002 (2013).
[20] K. Yagi and N. Yunes, I-Love-Q relations: From compact stars to black holes, Classical Quantum Gravity **33**, 095005 (2016).
[21] R. F. P. Mendes and H. Yang, Tidal deformability of dark matter clumps, Classical Quantum Gravity **34**, 185001 (2017).
[22] N. Uchikata, S. Yoshida, and P. Pani, Tidal deformability and I-Love-Q relations for gravastars with polytropic thin shells, Phys. Rev. D **94**, 064015 (2016).
[23] V. Cardoso, E. Franzin, A. Maselli, P. Pani, and G. Raposo, Testing strong-field gravity with tidal Love numbers, Phys. Rev. D **95**, 084014 (2017).
[24] N. V. Krishnendu, K. G. Arun, and C. K. Mishra, Testing the Binary Black Hole Nature of a Compact Binary Coalescence, Phys. Rev. Lett. **119**, 091101 (2017).
[25] A. Maselli, P. Pani, V. Cardoso, T. Abdelsalhin, L. Gualtieri, and V. Ferrari, Probing Planckian corrections at the horizon scale with LISA binaries, arXiv:1703.10612.
[26] C. Palenzuela, L. Lehner, and S. L. Liebling, Orbital dynamics of binary boson star systems, Phys. Rev. D **77**, 044036 (2008).
[27] B. C. Mundim, A numerical study of boson star binaries, arXiv:1003.0239.
[28] B. P. Abbott *et al.* (LIGO Scientific and Virgo Collaborations), Obser-vation of Gravitational Waves from a Binary Black Hole Merger, Phys. Rev. Lett. **116**, 061102 (2016).
[29] B. P. Abbott *et al.* (LIGO Scientific and Virgo Collaborations), GW151226: Observation of Gravitational Waves from a 22-Solar-Mass Binary Black Hole Coalescence, Phys. Rev. Lett. **116**, 241103 (2016).
[30] B. P. Abbott *et al.* (LIGO Scientific and Virgo Collaborations), Binary Black Hole Mergers in the First Advanced LIGO Observing Run, Phys. Rev. X **6**, 041015 (2016).
[31] B. P. Abbott *et al.* (LIGO Scientific and Virgo Collaborations), Tests of General Relativity with GW150914, Phys. Rev. Lett. **116**, 221101 (2016).
[32] C. Chirenti and L. Rezzolla, Did GW150914 produce a rotating gravastar?, Phys. Rev. D **94**, 084016 (2016).
[33] R. Konoplya and A. Zhidenko, Detection of gravitational waves from black holes: Is there a window for alternative theories?, Phys. Lett. B **756**, 350 (2016).
[34] N. Yunes, K. Yagi, and F. Pretorius, Theoretical physics implications of the binary black-hole mergers GW150914 and GW151226, Phys. Rev. D **94**, 084002 (2016).
[35] K. R. Dienes, String theory and the path to unification: A review of recent developments, Phys. Rep. **287**, 447 (1997).
[36] R. Brito, V. Cardoso, and P. Pani, Massive spin-2 fields on black hole spacetimes: Instability of the Schwarzschild and Kerr solutions and bounds on the graviton mass, Phys. Rev. D **88**, 023514 (2013).
[37] Y. Decanini, A. Folacci, and M. Ould El Hadj, Waveforms produced by a scalar point particle plunging into a Schwarzschild black hole: Excitation of quasinormal modes and quasibound states, Phys. Rev. D **92**, 024057 (2015).
[38] V. Cardoso, E. Franzin, and P. Pani, Is the Gravitational-Wave Ringdown a Probe of the Event Horizon?, Phys. Rev. Lett. **116**, 171101 (2016); Erratum, Phys. Rev. Lett. **117**, 089902(E) (2016).
[39] V. Cardoso, S. Hopper, C. F. B. Macedo, C. Palenzuela, and P. Pani, Gravitational-wave signatures of exotic compact objects and of quantum corrections at the horizon scale, Phys. Rev. D **94**, 084031 (2016).
[40] J. Abedi, H. Dykaar, and N. Afshordi, Echoes from the Abyss: Evidence for Planck-scale structure at black hole horizons, arXiv:1612.00266.
[41] J. Abedi, H. Dykaar, and N. Afshordi, Echoes from the Abyss: The holiday edition!, arXiv:1701.03485.
[42] C. Barcelo, R. Carballo-Rubio, and L. J. Garay, Gravitational echoes from macroscopic quantum gravity effects, J. High Energy Phys. 05 (2017) 054.
[43] E. Maggio, P. Pani, and V. Ferrari, Exotic compact objects and how to quench their ergoregion instability, arXiv:1703.03696.
[44] S. W. Hawking, Breakdown of predictability in gravitational collapse, Phys. Rev. D **14**, 2460 (1976).
[45] T. G. Cowling, The nonradial oscillations of polytropic stars, Mon. Not. R. Astron. Soc. **101**, 367 (1941).
[46] R. Brustein and M. Schmidt-Sommerfeld, Universe explosions, J. High Energy Phys. 07 (2013) 047.
[47] E. S. C. Ching, P. T. Leung, A. Maassen van den Brink, W. M. Suen, S. S. Tong, and K. Young, Quasinormal mode expansion for waves in open systems, Rev. Mod. Phys. **70**, 1545 (1998).
[48] R. H. Price and V. Husain, Model for the Completeness of Quasinormal Modes of Relativistic Stellar Oscillations, Phys. Rev. Lett. **68**, 1973 (1992).
[49] N. Andersson, K. D. Kokkotas, and B. F. Schutz, Spacetime modes of relativistic stars, Mon. Not. R. Astron. Soc. **280**, 1230 (1996).
[50] G. Allen, N. Andersson, K. D. Kokkotas, and B. F. Schutz, Gravitational waves from pulsating stars: Evolving the perturbation equations for a relativistic star, Phys. Rev. D **58**, 124012 (1998).
[51] K. D. Kokkotas and B. G. Schmidt, Quasinormal modes of stars and black holes, Living Rev. Relativ. **2**, 2 (1999).
[52] H.-P. Nollert, Quasinormal modes: The characteristic "sound" of black holes and neutron stars, Classical Quantum Gravity **16**, R159 (1999).
[53] K. D. Kokkotas and N. Andersson, Oscillation and instabilities of relativistic stars, arXiv:gr-qc/0109054.
[54] P. Pani, E. Berti, V. Cardoso, Y. Chen, and R. Norte, Gravitational wave signatures of the absence of an event

horizon. I. Nonradial oscillations of a thin-shell gravastar, Phys. Rev. D **80**, 124047 (2009).
[55] J. J. Atick and E. Witten, The Hagedorn transition and the number of degrees of freedom in string theory, Nucl. Phys. **B310**, 291 (1988).
[56] P. Salomonson and B.-S. Skagerstam, On superdense superstring gases: A heretic string model approach, Nucl. Phys. **B268**, 349 (1986).
[57] D. A. Lowe and L. Thorlacius, Hot string soup, Phys. Rev. D **51**, 665 (1995).
[58] L. Lindblom, B. J. Owen, and S. M. Morsink, Gravitational Radiation Instability in Hot Young Neutron Stars, Phys. Rev. Lett. **80**, 4843 (1998).
[59] P. Kovtun, D. T. Son, and A. O. Starinets, Viscosity in Strongly Interacting Quantum Field Theories from Black Hole Physics, Phys. Rev. Lett. **94**, 111601 (2005).
[60] E. Berti, J. Cardoso, V. Cardoso, and M. Cavaglia, Matched-filtering and parameter estimation of ringdown waveforms, Phys. Rev. D **76**, 104044 (2007).
[61] E. Berti, V. Cardoso, and C. M. Will, On gravitational-wave spectroscopy of massive black holes with the space interferometer LISA, Phys. Rev. D **73**, 064030 (2006).
[62] E. Berti, V. Cardoso, J. A. Gonzalez, U. Sperhake, M. Hannam, S. Husa, and B. Bruegmann, Inspiral, merger and ringdown of unequal mass black hole binaries: A multipolar analysis, Phys. Rev. D **76**, 064034 (2007).
[63] C. Cutler and E. E. Flanagan, Gravitational waves from merging compact binaries: How accurately can one extract the binary's parameters from the inspiral wave form?, Phys. Rev. D **49**, 2658 (1994).
[64] B. P. Abbott *et al.* (LIGO Scientific and Virgo Collaborations), Characterization of transient noise in Advanced LIGO relevant to gravitational wave signal GW150914, Classical Quantum Gravity **33**, 134001 (2016).
[65] P. Ajith, Addressing the spin question in gravitational-wave searches: Waveform templates for inspiralling compact binaries with nonprecessing spins, Phys. Rev. D **84**, 084037 (2011).
[66] E. Berti, A. Sesana, E. Barausse, V. Cardoso, and K. Belczynski, Spectroscopy of Kerr Black Holes with Earth- and Space-Based Interferometers, Phys. Rev. Lett. **117**, 101102 (2016).
[67] G. Ashton *et al.*, Comments on: "Echoes from the abyss: Evidence for Planck-scale structure at black hole horizons", arXiv:1612.05625.
[68] S. Bhagwat, D. A. Brown, and S. W. Ballmer, Spectroscopic analysis of stellar mass black-hole mergers in our local universe with ground-based gravitational wave detectors, Phys. Rev. D **94**, 084024 (2016); Erratum, Phys. Rev. D **95**, 069906(E) (2017).
[69] H. Yang, K. Yagi, J. Blackman, L. Lehner, V. Paschalidis, F. Pretorius, and N. Yunes, Black Hole Spectroscopy With Coherent Mode Stacking, Phys. Rev. Lett. **118**, 161101 (2017).
[70] V. Cardoso, L. C. B. Crispino, C. F. B. Macedo, H. Okawa, and P. Pani, Light rings as observational evidence for event horizons: Long-lived modes, ergoregions and nonlinear instabilities of ultracompact objects, Phys. Rev. D **90**, 044069 (2014).
[71] E. Barausse, V. Cardoso, and P. Pani, Environmental effects for gravitational-wave astrophysics, J. Phys. Conf. Ser. **610**, 012044 (2015).
[72] E. Barausse, V. Cardoso, and P. Pani, Can environmental effects spoil precision gravitational-wave astrophysics?, Phys. Rev. D **89**, 104059 (2014).
[73] R. Brustein and A. J. M. Medved, Quantum hair of black holes out of equilibrium, arXiv:1709.03566.
[74] G. T. Horowitz and J. Polchinski, Self-gravitating fundamental strings, Phys. Rev. D **57**, 2557 (1998).
[75] T. Damour and G. Veneziano, Self-gravitating fundamental strings and black holes, Nucl. Phys. **B568**, 93 (2000).
[76] P. J. Flory, *Principles of Polymer Chemistry* (Cornell University, Ithaca, New York, 1953).
[77] P. G. De Gennes, *Scaling Concepts in Polymer Physics* (Cornell University, Ithaca, New York, 1979).
[78] M. Doi and S. F. Edwards, *The Theory of Polymer Dynamics* (Oxford University Press, Oxford, 1986).
[79] P. G. De Gennes, Collapse of a polymer chain in poor solvents, J. Phys. Lett. **36**, L55 (1975).
[80] C. Williams, F. Brochard, and H. L. Frisch, Polymer Collapse, Annu. Rev. Phys. Chem. **32**, 433 (1981).
[81] R. A. Konoplya and A. Zhidenko, Quasinormal modes of black holes: From astrophysics to string theory, Rev. Mod. Phys. **83**, 793 (2011).
[82] L. Motl, An analytical computation of asymptotic Schwarzschild quasinormal frequencies, Adv. Theor. Math. Phys. **6**, 1135 (2002).
[83] B. F. Schutz and C. M. Will, Black hole normal modes: A semianalytic approach, Astrophys. J. **291**, L33 (1985).
[84] B. S. Sathyaprakash and B. F. Schutz, Physics, astrophysics and cosmology with gravitational waves, Living Rev. Relativ. **12**, 2 (2009).
[85] A Settimi *et al.*, Quasinormal-mode description of waves in one-dimensional photonic crystals, Phys. Rev. E **68**, 026614 (2003).
[86] A. Neitzke, Greybody factors at large imaginary frequencies, arXiv:hep-th/0304080.
[87] K. D. Kokkotas and B. F. Schutz, Normal modes of a model radiating system, Gen. Relativ. Gravit. **18**, 913 (1986).
[88] K. D. Kokkotas and B. F. Schutz, W-modes: A new family of normal modes of pulsating relativistic stars, Mon. Not. R. Astron. Soc. **255**, 119 (1992).
[89] N. Andersson, Y. Kojima, and K. D. Kokkotas, On the oscillation spectra of ultracompact stars: An extensive survey of gravitational-wave modes, Astrophys. J. **462**, 855 (1996).
[90] K. S. Thorne, Multipole expansion of gravitational radiation, Rev. Mod. Phys. **52**, 299 (1980).